HHS Public Access

Author manuscript

Biochem Pharmacol. Author manuscript; available in PMC 2019 November 17.

Published in final edited form as:

Biochem Pharmacol. 2018 February ; 148: 13–26. doi:10.1016/j.bcp.2017.11.022.

Targeting PI3K, mTOR, ERK, and Bcl-2 signaling network shows superior antileukemic activity against AML *ex vivo*

Yongwei Su[a,1], **Xinyu Li**[a,1], **Jun Ma**[a], **Jianyun Zhao**[a,b,e], **Shuang Liu**[a,b], **Guan Wang**[a], **Holly Edwards**[c,d], **Jeffrey W. Taub**[b,e], **Hai Lin**[f,*], **Yubin Ge**[c,d,e,*]

[a]National Engineering Laboratory for AIDS Vaccine, Key Laboratory for Molecular Enzymology and Engineering, the Ministry of Education, School of Life Sciences, Jilin University, Changchun, PR China

[b]Division of Pediatric Hematology/Oncology, Children's Hospital of Michigan, Detroit, MI, USA

[c]Department of Oncology, Wayne State University School of Medicine, Detroit, MI, USA

[d]Molecular Therapeutics Program, Barbara Ann Karmanos Cancer Institute, Wayne State University School of Medicine, Detroit, MI, USA

[e]Department of Pediatrics, Wayne State University School of Medicine, Detroit, MI, USA

[f]Department of Hematology and Oncology, The First Hospital of Jilin University, Changchun, PR China

Abstract

Acute myeloid leukemia (AML) remains challenging to treat and needs more effective treatments. The PI3K/mTOR pathway is involved in cell survival and has been shown to be constitutively active in 50–80% of AML patients. However, targeting the PI3K/mTOR pathway results in activation of the ERK pathway, which also plays an important role in cell survival. In addition, AML cells often overexpress antiapoptotic Bcl-2 family proteins (e.g., Bcl-2), preventing cell death. Thus, our strategy here is to target the PI3K, mTOR (by VS-5584, a PI3K and mTOR dual inhibitor), ERK (by SCH772984, an ERK-selective inhibitor), and Bcl-2 (by ABT-199, a Bcl-2-selective inhibitor) signaling network to kill AML cells. In this study, we show that while inhibition of PI3K, mTOR, and ERK showed superior induction of cell death compared to inhibition of PI3K and mTOR, the levels of cell death were modest in some AML cell lines and primary patient samples tested. Although simultaneous inhibition of PI3K, mTOR, and ERK caused downregulation of Mcl-1 and upregulation of Bim, immunoprecipitation of Bcl-2 revealed increased binding of Bim to Bcl-2, which was abolished by the addition of ABT-199, suggesting that Bim was bound to Bcl-2 which prevented cell death. Treatment with combined VS-5584, SCH772984, and ABT-199 showed significant increase in cell death in AML cell lines and primary patient samples and significant reduction in AML colony formation in primary patient samples, while there was no significant effect on colony formation of normal human CD34+

[*]Corresponding authors at: Department of Oncology, Wayne State University School of Medicine, 421 E. Canfield, Detroit, MI 48201, USA (Y. Ge). maillinhai@sina.com (H. Lin), gey@karmanos.org (Y. Ge).

[1]These authors contributed equally to this work.

Conflict of interest

The authors declare that they have no competing interests.

hematopoietic progenitor cells. Taken together, our findings show that inhibition of PI3K, mTOR, and ERK synergistically induces cell death in AML cells, and addition of ABT-199 enhances cell death further. Thus, our data support targeting the PI3K, mTOR, ERK, and Bcl-2 signaling network for the treatment of AML.

Keywords

Acute myeloid leukemia; PI3K; mTOR; ERK; Bcl-2

1. Introduction

Patients with acute myeloid leukemia (AML) have a dismal prognosis. The majority of AML patients who undergo standard induction therapy, consisting of cytarabine plus an anthracycline (e.g., daunorubicin), relapse. In addition, AML patients who are elderly or have co-morbidities do not tolerate standard induction therapy. Thus, more effective therapies with lower toxicities are desperately needed for the treatment of AML.

The PI3K/mTOR pathway, which is involved in cell survival, has been shown to be constitutively active in 50–80% of AML patients. While PI3K inhibitors have shown promising results in preclinical AML models, clinical results have been disappointing [1]. The first inhibitors developed to target this pathway were mTOR inhibitors. Unfortunately, mTOR inhibition, through induction of feedback loops, causes hyperactivation of PI3K [2,3]. Further, PI3K/mTOR inhibition has been shown to cause compensatory ERK activation, resulting in cell survival [2,4,5]. In addition, AML cells have also been shown to overexpress antiapoptotic Bcl-2 family proteins (e.g., Bcl-2), protecting them from cell death [6–10]. Although results from a Phase II AML clinical trial using the Bcl-2-selective inhibitor ABT-199 (Venetoclax) showed promising results, all the ABT-199 treated patients relapsed in a short period of time (median time to relapse was 2.5 months) [11]. Therefore, we hypothesize that targeting the PI3K, mTOR, ERK, and Bcl-2 signaling network would result in superior antileukemic activity against AML.

In this study, we show that inhibition of PI3K, mTOR, and ERK results in enhanced AML cell death. However, cell death induced by the combination was variable, ranging from 15% to 80% cell death. Cell death induced by combined inhibition of PI3K, mTOR, and ERK was mediated at least partially through upregulation of Bim and downregulation of Mcl-1. While cell death could be attributed to caspase activation early on, longer treatment revealed a lack of caspase dependence. Even though overall levels of Bim were increased, association with the antiapoptotic protein Bcl-2 was also increased, preventing apoptosis from occurring. As such, inhibition of Bcl-2 enhanced cell death induced by PI3K/mTOR and ERK inhibition in AML cells. Our findings support targeting multiple aspects of the survival signaling network to eliminate AML cells.

2. Materials and methods

2.1. Drugs

The PI3K and mTOR dual inhibitor VS-5584, the ERK-selective inhibitor SCH772984, the Bcl-2-selective inhibitor ABT-199, and CUDC-907 (a PI3K and HDAC dual inhibitor, used as a positive control in this study) were purchased from Selleck Chemicals (Houston, TX, USA). Z-VAD-FMK was purchased from Sigma-Aldrich (St. Louis, MO, USA).

2.2. Cell culture

MV4–11, THP-1, and U937 cell lines were purchased from the American Type Culture Collection (Manassas, VA, USA). The OCIAML3 cell line was purchased from the German Collection of Microorganisms and Cell Cultures (DSMZ, Braunschweig, Germany). Dr. A Fuse from the National Institute of Infectious Diseases (Tokyo, Japan) kindly gifted us the CMS and CTS cell lines. MOLM-13 cells were purchased from AddexBio (San Diego, CA, USA). The human AML cell lines were cultured as previously described [12]. Uphoff and Drexler's PCR based method was used monthly to test for mycoplasma [13]. Cell lines were authenticated in August 2017 at the Genomics Core at Karmanos Cancer Institute using the PowerPlex® 16 System from Promega (Madison, WI, USA).

Diagnostic AML blast samples derived from patients and peripheral blood mononuclear cells (PMNCs) from healthy donors were purified by standard Ficoll-Hypaque density centrifugation. Human CD34+ cord blood cells were purchased from Nuowei Biotechnology Co., Ltd (Beijing, China). Diagnostic AML blasts, normal PMNCs, and human CD34+ cord blood cells were cultured as previously described [12,14,15].

2.3. Clinical samples

Diagnostic AML blast samples were obtained from the First Hospital of Jilin University, Changchun, China. Written informed consent was provided according to the Declaration of Helsinki. This study was approved and carried out in accordance with the guidelines set forth by the Human Ethics Committee of the First Hospital of Jilin University. Clinical samples were screened for gene mutations and for fusion genes by real-time RT-PCR, as described previously [14,16]. See Table 1 for patient characteristics.

2.4. In vitro cytotoxicity assays

MTT (3-[4,5-dimethyl-thiazol-2-yl]-2,5-diphenyltetrazolium bromide, Sigma-Aldrich) assays were performed as previously described [12,17,18]. The cells were treated for 72 h. The IC_{50} values for the cell lines are presented as mean values ± SEM from at least three independent experiments. Due to limited sample, the IC_{50} values for the patient samples are means of duplicates from one experiment. Patient samples were chosen solely based on sample availability.

2.5. Western blot analysis

Western blot analysis was performed as previously described [12,17,19–21]. Western blots were immunoblotted with anti-PARP, -Mcl-1, -Bcl-2, -Bcl-xL, -Bax, -β-actin, -ERK, (Proteintech, Chicago, IL, USA), -p-AKT (T308), -p-AKT (S473) (Affinity Biosciences,

Zhenjiang, Jiangsu, China), -Bim, -cf-Caspase 3, -p-S6 (Cell Signaling Technologies, Danvers, MA, USA), -p-ERK (T202/Y204), -AKT, -Bak (Abcam, Cambridge, MA, USA) antibodies, as previously described. Western blots were performed at least 3 independent times, with the exception of the primary patient samples. Densitometry measurements were normalized to β-actin and then compared to vehicle-treated control. Representative blots are shown.

2.6. Annexin V/PI staining and flow cytometry analysis

AML cells were treated with VS-5584, SCH772984, Z-VAD-FMK, or ABT-199 alone or in combination for up to 48 h. Drug-induced apoptosis was determined using an Annexin V-fluorescein isothiocyanate (FITC)/propidium iodide PI) apoptosis Kit Beckman Coulter; Brea, CA, USA), as previously described [17,22,23]. For AML cell lines, experiments were performed 2 independent times in triplicates. Patient samples had limited number of cells and so patient sample experiments were performed once in triplicates. Apoptotic events are presented as mean percentage of Annexin V +/PI− and Annexin V+/PI+ ± SEM from one representative experiment. Synergy was determined by calculating the combination index (CI) values using CompuSyn software (Combosyn Inc., Paramus, NJ). CI < 1, CI = 1, and CI > 1 indicate synergistic, additive, and antagonistic effects, respectively.

2.7. Assessment of mitochondrial outer membrane potential (MOMP)

Mitochondrial outer membrane potential was determined as previously described [24,25].

2.8. Immunoprecipitation (IP)

Immunoprecipitation of Bim and Bcl-2 was performed as previously described [24,26] using 2 μg of anti-Bim (2819, Cell Signaling Technology) or anti-Bcl-2 (SC-819, Santa Cruz Biotechnology, Santa Cruz, CA) antibody, 1 mg protein lysate, and Protein A agarose beads (Roche Diagnostics).

2.9. shRNA knockdown of Bim and ectopic overexpression of Mcl-1

Dr. Dong at Tulane University provided the pMD-VSV-G and delta 8.2 plasmids. Bim and non-target control (NTC) shRNA lentiviral vectors were purchased from Sigma-Aldrich. Red fluorescent protein (RFP) and Mcl-1 cDNA constructs were purchased from Thermo Fisher Scientific Biosciences Lafayette, CO, USA). Lentivirus production and transduction were carried out using Lipofectamine and Plus reagents Life Technologies), as previously described [12,27].

2.10. Colony formation assay

Diagnostic AML blast samples and normal human CD34+ cord blood cells were pretreated with VS-5584 and SCH772984 alone or in combination for 12 h, then ABT-199 was added and the cells were incubated for an additional 12 h. The cells were washed with PBS three times and then plated in triplicate in MethoCult (Stem Cell Technologies, Cambridge, MA, USA) and incubated for 14 days, according to the manufacturer’s instructions. Colony forming units were visualized using an inverted microscope and the number of colonies was enumerated.

2.11. Statistical analysis

Differences in cell death between treated (individually or combined) and untreated cells or combined and individual drug treatment were compared using the pair-wise two-sample *t*-test. Differences in VS-5584 IC_{50}s between FLT3-ITD vs. Non-FLT3-ITD were calculated using the Mann-Whitney *U* test. Statistical analyses were performed with GraphPad Prism 5.0. Error bars represent ± SEM. The level of significance was set at $p < .05$.

3. Results

3.1. The PI3K/mTOR dual inhibitor VS-5584 induces proliferation arrest and caspase-independent cell death in AML cell lines

To begin our investigation, we used MTT assays to determine AML cell line and primary patient sample sensitivities to the PI3K/mTOR dual inhibitor VS-5584. VS-5584 IC_{50}s ranged from 303 nM to 1.4 μM in the cell lines and from 7 nM to 5.3 μM in the primary AML patient samples (n = 43, median IC_{50} was 1.1 μM, Fig. 1A, B). There did not appear to be a difference between VS and 5584 IC_{50}s in the AML patient samples with or without FLT3-ITD (median IC50s were 1.07 and 1.02 μM, respectively, p = .601, Fig. 1C). Next, we determined the effects of VS-5584 treatment on cell death. AML cell lines were treated with variable concentrations of VS-5584 for 48 h and then subjected to Annexin V/PI staining and flow cytometry analysis. VS-5584-induced cell death among the cell lines varied (Fig. 1D, E); 2 μM VS-5584 induced little to no cell death in the THP-1 cells, while inducing 39% cell death in the MV4–11 cells. In MOLM-13 cells, VS-5584 treatment caused neither cleavage of caspase 3 and PARP (Fig. 1F) nor a loss of mitochondrial outer membrane potential (MOMP; Fig. 1G), suggesting that cell death-induced by VS-5584 in MOLM-13 cells was caspase-independent. Interestingly, addition of the pan-caspase inhibitor Z-VAD-FMK to VS-5584 treatment did not rescue the cells, rather it enhanced cell death induced by VS-5584 (Fig. 1H). Time course results show that VS-5584 induced appreciable level of cell death by 24 h (Fig. 1I). Similar to the 48 h treatment, the pan-caspase inhibitor enhanced VS-5584-induced cell death after 24 h treatment as well (Fig. 1J). In contrast, the pan-caspase inhibitor was able to partially reduce cell death induced by the Bcl-2-selective inhibitor ABT-199 in MOLM-13 cells (Fig. 1K). While VS-5584 treatment did result in caspase 3 and PARP cleavage, as well as decrease in MOMP in CMS cells, treatment with the pancaspase inhibitor enhanced VS-5584-induced cell death (data not shown). Taken together, these results suggest that VS-5584 induces caspase-independent cell death in AML cells.

3.2. VS-5584 treatment results in ERK activation which can be abolished by the ERK-selective inhibitor SCH772984 resulting in synergistic induction of cell death in AML cell lines

To determine if VS-5584 inhibited both PI3K and mTOR, MOLM-13, U937, and THP-1 cells were treated with variable concentrations of VS-5584 and then whole cell lysates were subjected to Western blotting. As expected, VS-5584 treatment resulted in significant downregulation of p-AKT (T308), p-AKT (S473), and p-S6, confirming that both PI3K and mTOR were inhibited in these cells (Fig. 2A). Interestingly, VS-5584 treatment also caused a decrease in total AKT in the MOLM-13 cells. Downregulation of p-AKT and p-S6 could

be detected in MOLM-13 and CMS cells as early as 3 h post-VS-5584 treatment (data not shown). VS-5584 treatment caused a concentration-dependent significant increase in p-ERK, indicating activation of the ERK pathway in the AML cell lines tested (Fig. 2A). Given the critical role ERK plays in cell survival [4], our results suggest that ERK activation in response to VS-5584 treatment attenuates cell death induced by VS-5584. To overcome this, we treated the AML cell lines with VS-5584 alone and in combination with the ERK-selective inhibitor SCH772984. Western blot analysis revealed that SCH772984 abrogated the increase in p-ERK in response to VS-5584 treatment and reduced total ERK levels (Fig. 2B). Treatment with SCH772984 decreased p-AKT (S473) and p-AKT (T308) in U937 cells, while levels remained unchanged in the MOLM-13 and THP-1 cells. After combined VS-5584 and SCH772984 treatment, p-AKT (S473) and p-AKT (T308) levels were similar to or less than VS-5584 treatment alone in all three cell lines. p-S6 levels were decreased after SCH772984 treatment in U937 and THP-1 cells, while levels remained unchanged in the MOLM-13 cells. The combined treatment resulted in decreased p-S6 levels compared to individual treatment in both MOLM-13 and THP-1 cells, but not in U937 cells, in which VS-5584 treatment almost completed abolished p-S6 expression (Fig. 2B). These molecular changes were accompanied by synergistic induction of cell death induced by the two agents in the MOLM-13, U937, and THP-1 cells, and in 4 additional AML cell lines (Fig. 2C). It is important to note that although VS-5584 and SCH772984 synergized in inducing cell death in THP-1 cells, the levels were minimal (about 15%), suggesting that there may be other factors preventing cell death induced by the combination of the two agents.

3.3. Combined treatment with VS-5584 and SCH772984 results in both caspase-dependent and independent cell death in AML cell lines

Combined VS-5584 and SCH772984 treatment for 48 h resulted in cleavage of caspase 3 and PARP, and loss of MOMP in MOLM-13 cells (Fig. 3A, B). However, the pan-caspase inhibitor Z-VAD-FMK did not rescue the cells. In fact, it enhanced cell death induced by the combined treatment, suggesting that cell death induced by the combination was at least partially caspase-independent (Fig. 3C, D). Time course results showed induction of cell death as early as 6 h post combined VS-5584 and SCH772984 treatment (Fig. 3E). To determine if caspase activation was required in cell death induced by the combination at an early time, MOLM-13 cells were treated with combined VS-5584 and SCH772984, along with Z-VAD-FMK for 12 h, and then the cells were subjected to Annexin V/PI staining and flow cytometry analysis. Interestingly, Z-VADFMK partially rescued the cells, especially Annexin V+/PI- cells (Fig. 3F). Similar results were also obtained in MV4–11 cells (Fig. 3G). Combined VS-5584 and SCH772984 treatment for 12 h did not cause a significant loss in MOMP, though caspase 3 cleavage was detected (data not shown), indicating that cell death may have been mediated through the extrinsic apoptosis pathway. These results suggest that cell death induced by the combination of VS-5584 and SCH772984 was partially caspase-dependent, though given enough time cell death occurred independent of caspase.

3.4. VS-5584 and SCH772984 synergizes in causing proliferation arrest and cell death in primary AML patient samples but not in normal human PMNCs

Next we tested the combination of VS-5584 and SCH772984 in primary AML patient samples. Western blotting of one primary AML patient sample (AML#40) showed a decrease in p-AKT (T308), p-AKT (S473), total AKT, and p-S6 following VS-5584 treatment for 48 h (Fig. 4A). In agreement with the cell line data, p-ERK levels were increased following VS-5584 treatment, while combined treatment with SCH772984 showed levels comparable to SCH772984 treatment alone. Similar to the cell line data, SCH772984 treatment reduced total ERK levels, which was maintained in the combined treatment. Flow cytometry analysis revealed synergistic induction of cell death in 2 primary AML patient samples, however the levels of cell death were modest (20–35%, Fig. 4B, C). Due to limited sample, the combination was tested in an additional 11 primary AML patient samples by MTT assays. The combined treatment resulted in synergistic reduction in viable cells in all 11 primary AML patient samples (Fig. 4D). The drug treatments were then tested in normal PMNCs. As shown in Fig. 4E, individual and combined drug treatments showed little to no effect on the percentage of viable cells in normal human PMNCs (Fig. 4E). These results demonstrate that VS-5584 and SCH772984 synergizes in inducing cell death and proliferation inhibition in primary AML patient samples but not in normal human PMNCs.

3.5. Bcl-2, Mcl-1, and Bim play important roles in cell death induced by the combination of VS-5584 and SCH772984 in AML cells

The PI3K/mTOR and ERK pathways have both been shown to regulate Bcl-2 family proteins [28–33]. It is conceivable that the combination of VS-5584 and SCH772984 induces cell death through modulation of Bcl-2 family proteins in AML cells. To test this possibility, MOLM-13 cells were treated with the two drugs alone and in combination for 48 h. VS-5584 treatment significantly decreased Mcl-1 level, while SCH772984 treatment significantly increased Bim level (Fig. 5A). In the combined treatment, Mcl-1 levels were further decreased and Bim levels were further increased compared to individual drug treatment. In contrast, protein levels for Bax, Bcl-2, Bak, and Bcl-xL remain largely unchanged (Fig. 5A). Significant Mcl-1 downregulation and Bim upregulation were detected as early as 3 h post-treatment in MOLM-13 cells (Fig. 5B) and around 6–12 h in CMS cells (data not shown). Significantly decreased Mcl-1 was detected in 3 additional AML cell lines post-VS-5584 and combined drug treatment for 12 h (compared to vehicle control), while significantly increased Bim levels were detected after combined drug treatment (Fig. 5C). shRNA knockdown of Bim significantly reduced cell death induced by VS-5584 alone and in combination with SCH772984 post-12 h treatment. However, there was no significant difference between drug-induced cell death 48 h post-drug treatment (Fig. 5D). Mcl-1 overexpression had a slight yet significant impact on VS-5584 treatment alone and in combination for 12 and 48 h (Fig. 5E). These results suggest that Bim and Mcl-1 play an important role in cell death induced by the combination during the early hours of treatment. However, as exemplified by THP-1 cells (Fig. 2C) and two primary AML patient samples (AML#40 and AML#42, Fig. 4B, C), the extent of cell death induced by the combination was modest, suggesting that although Bim levels increased, Bim may have been prevented from inducing cell death by interacting with antiapoptotic Bcl-2 family proteins (e.g., Bcl-2).

To determine if inhibition of Bcl-2 enhances cell death induced by the combination of VS-5584 and SCH772984, we treated THP-1 cells with VS-5584 and SCH772984 in combination for 12 h, then added ABT-199 and incubated the cells for an additional 12 h (Fig. 6A). Addition of ABT-199 reduced Mcl-1 levels below combined VS-5584 and SCH-772984 treatment, while Bim levels were similar to the combined treatment. Consistent with our previous report [24], ABT-199 treatment resulted in an increase in Mcl-1 in the cells (Fig. 6B). Immunoprecipitation of Bcl-2 revealed increased binding of Bim to Bcl-2 in AML cells post combined VS-5584 and SCH772984 treatment, which was abolished by the addition of ABT-199, suggesting that the increased Bim was bound to Bcl-2 which prevented cell death (Fig. 6C). Reciprocal immunoprecipitation of Bim showed increased binding to Bcl-2, which was not observed in the three drug combination (Fig. 6D). Consistent with our previous findings [24], Mcl-1 association with Bim increased following ABT-199 treatment, but was abolished by the three drug combination. While the three drug combination resulted in increased Bim in the whole cell lysate (Fig. 6B), increased Bim was not detected following immunoprecipitation of Bim (Fig. 6D). We speculate that this may be due to a conformational change which interfered with the immunoprecipitation of Bim. Interestingly, the three drug combination induced significantly more cell death compared to control, single drug treatment, or any of the two drug combinations in THP-1 cells, along with 3 additional AML cell lines (Fig. 6E). shRNA knockdown of Bim significantly reduced cell death induced by the three drug combination (Fig. 6F, G) and was at least partially caspase dependent (Fig. 6H), suggesting that Bim plays an important role in cell death induced by the three drug combination.

3.6. The combination of VS-5584, SCH772984, and ABT-199 shows superior antileukemic activities against primary AML blasts but spares normal hematopoietic progenitor cells

Finally, we tested the three drug combination in 6 primary AML patient samples *ex vivo*. Annexin V/PI staining and flow cytometry analysis revealed that ABT-199 significantly enhanced cell death induced by combined VS-5584 and SCH772984 treatment (Fig. 7A). To determine the effects of drug treatment on leukemia progenitor cells, primary AML patient samples were treated with VS-5584, SCH772984, and ABT-199, alone or in combination, for up to 24 h, and then plated in methylcellulose, and incubated for 2 weeks. Simultaneous inhibition of PI3K/mTOR and ERK, followed by inhibition of Bcl-2 significantly reduced the number of AML-CFUs (Fig. 7B). The same experiment was performed in human CD34+ cord blood cells to assess the effects of these treatments on normal hematopoietic progenitor cells. Results show no significant effect on colony formation, suggesting that the three drug combination spares normal hematopoietic progenitor cells (Fig. 7C, D). Taken together, our findings show that VS-5584 and SCH772984 synergistically induce cell death in AML cells, which can be further enhanced by inhibition of Bcl-2 with its selective inhibitor ABT-199.

4. Discussion

Many studies have shown that targeting PI3K, mTOR, ERK, or Bcl-2 can result in intrinsic or acquired resistance to the corresponding inhibitors mediated through other survival pathways [2,3,34–37]. The PI3K/mTOR pathway is involved in many cellular processes, including cell survival, and is constitutively active in the majority of AML patients [38–40],

making it an attractive target for the treatment of AML. However, we and others have shown that dual inhibition of PI3K and mTOR can cause increased activation of ERK [21,34–36], which prompted investigations into combined inhibition of the PI3K/mTOR and ERK pathways for cancer treatment. In agreement with those studies, we found that combined inhibition of PI3K, mTOR, and ERK resulted in synergistic induction of AML cell death (Fig. 2C). However, as exemplified by the THP-1 cells (Fig. 2C) and primary AML patient samples (AML#40 and AML#42, Fig. 4B, C), response to combined inhibition was modest (Fig. 4). Moreover, other published works show variable induction of cell death induced by combined inhibition of both the PI3K/mTOR and ERK pathways [34,36], supporting the possibility that other survival pathways may be preventing drug-induced cell death.

PI3K inhibition has been shown to decrease the antiapoptotic protein Mcl-1 [41], which we confirmed in AML cells (Fig. 5A). Inhibition of PI3K and ERK have been shown to downregulate Mcl-1 through degradation and regulation of Mcl-1 transcription [34,41]. Thus, combined inhibition of PI3K, mTOR, and ERK likely caused downregulation of Mcl-1 through both transcriptional and posttranscriptional mechanisms. In agreement with published reports [31,32], we show that ERK inhibition upregulates Bim and inhibition of PI3K and mTOR further increases Bim levels. In B-cell acute lymphoblastic leukemia, it has been demonstrated that inhibition of ERK1/2 results in upregulation of Bim and increased binding of Bim to Mcl-1, preventing cell death [33]. In contrast, we detected upregulation of Bim and downregulation of Mcl-1. However, similar to their findings, we did detect increased binding of Bim to another antiapoptotic protein, Bcl-2. Thus, inhibition of PI3K, mTOR and ERK likely leaves other antiapoptotic Bcl-2 family proteins available to interact with Bim and prevent cell death.

Inhibition of PI3K/mTOR and the Bcl-2 pathway was shown by Rahmani and colleagues to have promising antileukemic activity in AML cell lines and in an AML xenograft model [42]. In their study, they found that the dual PI3K/mTOR inhibitor BEZ235 and the Bcl-2/Bcl-xL inhibitor ABT-737 induce apoptosis in AML cells. Similar to our findings, they also found that downregulation of Mcl-1 and upregulation of Bim contributed to combined inhibition of Bcl-2 and PI3K/mTOR. They found that combined inhibition showed response in 4 of 6 AML patient samples tested, demonstrating that there were some resistant samples. In a similar fashion, we found variable induction of cell death in AML cells treated simultaneously with PI3K/mTOR and Bcl-2 inhibitor ABT-199. BEZ235 has been shown by others to result in activation of the MEK/ERK pathway [36]. Our study incorporates this finding and shows that inhibition of PI3K/mTOR and Bcl-2 in AML cells can be enhanced by ERK inhibition, which builds upon the findings of Rahmani et al.

The combined inhibition of PI3K, mTOR, ERK, and Bcl-2 not only showed activity against bulk leukemia cells but also leukemia progenitor cells. Our results show that simultaneous inhibition of PI3K, mTOR, and ERK followed by inhibition of Bcl-2 significantly reduced the number of AML-CFUs and spared normal hematopoietic progenitor cells, suggesting that targeting all three pathways resulted in superior antileukemic activity. Although, further *in vivo* testing is warranted to determine the effects of targeting the PI3K, mTOR, ERK, and Bcl-2 signaling network on AML cells, including leukemia progenitor cells. In conclusion, our results show that inhibition of PI3K and mTOR causes ERK activation in AML cells and

while inhibition of ERK enhances AML cell death induced by combined inhibition of PI3K and mTOR, Bcl-2 inhibition further enhances cell death. The data presented provide compelling support for the strategy of inhibiting PI3K, mTOR, ERK, and Bcl-2 signaling network for the treatment of AML.

Acknowledgements

This study was supported by Jilin University, Changchun, China, the Barbara Ann Karmanos Cancer Institute, Wayne State University School of Medicine, and by grants from the National Natural Science Foundation of China, NSFC 31671438 and NSFC 31471295, China Scholar Council, Hyundai Hope on Wheels, LaFontaine Family/U Can-Cer Vive Foundation, Kids Without Cancer, Children's Hospital of Michigan Foundation, Decerchio/Guisewite Family, Justin's Gift, Elana Fund, Ginopolis/Karmanos Endowment and the Ring Screw Textron Endowed Chair for Pediatric Cancer Research. The Genomics Core is supported, in part, by NIH Center Grant P30 CA022453 to the Karmanos Cancer Institute at Wayne State University. The funders had no role in study design, data collection, analysis and interpretation of data, decision to publish, or preparation of the manuscript.

References

[1]. Fransecky L, Mochmann LH, Baldus CD, Outlook on PI3K/AKT/mTOR inhibition in acute leukemia, Mol. Cell Ther 3 (2015) 2. [PubMed: 26056603]

[2]. Rozengurt E, Soares HP, Sinnet-Smith J, Suppression of feedback loops mediated by PI3K/mTOR induces multiple overactivation of compensatory pathways: an unintended consequence leading to drug resistance, Mol. Cancer Ther. 13 (2014) 2477–2488. [PubMed: 25323681]

[3]. O'Reilly KE, Rojo F, She QB, Solit D, Mills GB, Smith D, Lane H, Hofmann F, Hicklin DJ, Ludwig DL, Baselga J, Rosen N, mTOR inhibition induces upstream receptor tyrosine kinase signaling and activates Akt, Cancer Res. 66 (2006) 1500–1508. [PubMed: 16452206]

[4]. Samatar AA, Poulikakos PI, Targeting RAS-ERK signalling in cancer: promises and challenges, Nat. Rev. Drug Discov 13 (2014) 928–942. [PubMed: 25435214]

[5]. Caunt CJ, Sale MJ, Smith PD, Cook SJ, MEK1 and MEK2 inhibitors and cancer therapy: the long and winding road, Nat. Rev. Cancer 15 (2015) 577–592. [PubMed: 26399658]

[6]. Saxena A, Viswanathan S, Moshynska O, Tandon P, Sankaran K, Sheridan DP, Mcl-1 and Bcl-2/Bax ratio are associated with treatment response but not with Rai stage in B-cell chronic lymphocytic leukemia, Am. J. Hematol 75 (2004) 22–33. [PubMed: 14695629]

[7]. Lauria F, Raspadori D, Rondelli D, Ventura MA, Fiacchini M, Visani G, Forconi F, Tura S, High bcl-2 expression in acute myeloid leukemia cells correlates with CD34 positivity and complete remission rate, Leukemia 11 (1997) 2075–2078. [PubMed: 9447823]

[8]. Keith FJ, Bradbury DA, Zhu YM, Russell NH, Inhibition of bcl-2 with antisense oligonucleotides induces apoptosis and increases the sensitivity of AML blasts to Ara-C, Leukemia 9 (1995) 131–138. [PubMed: 7845007]

[9]. Schimmer AD, O'Brien S, Kantarjian H, Brandwein J, Cheson BD, Minden MD, Yee K, Ravandi F, Giles F, Schuh A, Gupta V, Andreeff M, Koller C, Chang H, Kamel-Reid S, Berger M, Viallet J, Borthakur G, A phase I study of the pan bcl-2 family inhibitor obatoclax mesylate in patients with advanced hematologic malignancies, Clin. Cancer Res. 14 (2008) 8295–8301. [PubMed: 19088047]

[10]. Fennell DA, Corbo MV, Dean NM, Monia BP, Cotter FE, In vivo suppression of Bcl-XL expression facilitates chemotherapy-induced leukaemia cell death in a SCID/NOD-Hu model, Br. J. Haematol 112 (2001) 706–713. [PubMed: 11260076]

[11]. Konopleva M, Pollyea DA, Potluri J, Chyla B, Hogdal L, Busman T, McKeegan E, Salem AH, Zhu M, Ricker JL, Blum W, DiNardo CD, Kadia T, Dunbar M, Kirby R, Falotico N, Leverson J, Humerickhouse R, Mabry M, Stone R, Kantarjian H, Letai A, Efficacy and biological correlates of response in a phase II study of venetoclax monotherapy in patients with acute myelogenous leukemia, Cancer Discov 6 (2016) 1106–1117. [PubMed: 27520294]

[12]. Zhao J, Niu X, Li X, Edwards H, Wang G, Wang Y, Taub JW, Lin H, Ge Y, Inhibition of CHK1 enhances cell death induced by the Bcl-2-selective inhibitor ABT-199 in acute myeloid leukemia cells, Oncotarget 7 (2016) 34785–34799. [PubMed: 27166183]

[13]. Uphoff CC, Drexler HG, Detection of mycoplasma contaminations, Methods Mol. Biol 290 (2005) 13–23. [PubMed: 15361652]

[14]. Niu X, Wang G, Wang Y, Caldwell JT, Edwards H, Xie C, Taub JW, Li C, Lin H, Ge Y, Acute myeloid leukemia cells harboring MLL fusion genes or with the acute promyelocytic leukemia phenotype are sensitive to the Bcl-2-selective inhibitor ABT-199, Leukemia 28 (2014) 1557–1560. [PubMed: 24531733]

[15]. Taub JW, Matherly LH, Stout ML, Buck SA, Gurney JG, Ravindranath Y, Enhanced metabolism of 1-beta-D-arabinofuranosylcytosine in Down syndrome cells: a contributing factor to the superior event free survival of Down syndrome children with acute myeloid leukemia, Blood 87 (1996) 3395–3403. [PubMed: 8605357]

[16]. Qi W, Xie C, Li C, Caldwell JT, Edwards H, Taub JW, Wang Y, Lin H, Ge Y, CHK1 plays a critical role in the anti-leukemic activity of the wee1 inhibitor MK-1775 in acute myeloid leukemia cells, J. Hematol. Oncol 7 (2014) 53. [PubMed: 25084614]

[17]. Xie C, Edwards H, Xu X, Zhou H, Buck SA, Stout ML, Yu Q, Rubnitz JE, Matherly LH, Taub JW, Ge Y, Mechanisms of synergistic antileukemic interactions between valproic acid and cytarabine in pediatric acute myeloid leukemia, Clin. Cancer Res 16 (2010) 5499–5510. [PubMed: 20889917]

[18]. Xu X, Xie C, Edwards H, Zhou H, Buck SA, Ge Y, Inhibition of histone deacetylases 1 and 6 enhances cytarabine-induced apoptosis in pediatric acute myeloid leukemia cells, PLoS One 6 (2011) e17138. [PubMed: 21359182]

[19]. Ge Y, Dombkowski AA, LaFiura KM, Tatman D, Yedidi RS, Stout ML, Buck SA, Massey G, Becton DL, Weinstein HJ, Ravindranath Y, Matherly LH, Taub JW, Differential gene expression, GATA1 target genes, and the chemotherapy sensitivity of Down syndrome megakaryocytic leukemia, Blood 107 (2006) 1570–1581. [PubMed: 16249385]

[20]. Ge Y, Stout ML, Tatman DA, Jensen TL, Buck S, Thomas RL, Ravindranath Y, Matherly LH, Taub JW, GATA1, cytidine deaminase, and the high cure rate of Down syndrome children with acute megakaryocytic leukemia, J. Natl. Cancer Inst. 97 (2005) 226–231. [PubMed: 15687366]

[21]. Ning C, Liang M, Liu S, Wang G, Edwards H, Xia Y, Polin L, Dyson G, Taub JW, Mohammad RM, Azmi AS, Zhao L, Ge Y, Targeting ERK enhances the cytotoxic effect of the novel PI3K and mTOR dual inhibitor VS-5584 in preclinical models of pancreatic cancer, Oncotarget 8 (2017) 44295–44311. [PubMed: 28574828]

[22]. Edwards H, Xie C, LaFiura KM, Dombkowski AA, Buck SA, Boerner JL, Taub JW, Matherly LH, Ge Y, RUNX1 regulates phosphoinositide 3-kinase/AKT pathway: role in chemotherapy sensitivity in acute megakaryocytic leukemia, Blood 114 (2009) 2744–2752. [PubMed: 19638627]

[23]. Zhao J, Xie C, Edwards H, Wang G, Taub JW, Ge Y, Histone deacetylases 1 and 2 cooperate in regulating BRCA1, CHK1, and RAD51 expression in acute myeloid leukemia cells, Oncotarget 8 (2017) 6319–6329. [PubMed: 28030834]

[24]. Niu X, Zhao J, Ma J, Xie C, Edwards H, Wang G, Caldwell JT, Xiang S, Zhang X, Chu R, Wang ZJ, Lin H, Taub JW, Ge Y, Binding of released Bim to Mcl-1 is a mechanism of intrinsic resistance to ABT-199 which can be overcome by combination with daunorubicin or cytarabine in AML cells, Clin. Cancer Res. 22 (2016) 4440–4451. [PubMed: 27103402]

[25]. Xie C, Edwards H, Caldwell JT, Wang G, Taub JW, Ge Y, Obatoclax potentiates the cytotoxic effect of cytarabine on acute myeloid leukemia cells by enhancing DNA damage, Mol. Oncol 9 (2015) 409–421. [PubMed: 25308513]

[26]. Luedtke DA, Niu X, Pan Y, Zhao J, Liu S, Edwards H, Chen K, Lin H, Taub JW, Ge Y, Inhibition of Mcl-1 enhances cell death induced by the Bcl-2-selective inhibitor ABT-199 in acute myeloid leukemia cells, Signal Trans. Targ. Therap 2 (2017) 17012.

[27]. Xie C, Drenberg C, Edwards H, Caldwell JT, Chen W, Inaba H, Xu X, Buck SA, Taub JW, Baker SD, Ge Y, Panobinostat enhances cytarabine and daunorubicin sensitivities in AML cells through suppressing the expression of BRCA1, CHK1, and Rad51, PLoS one 8 (2013) e79106. [PubMed: 24244429]

[28]. Steelman LS, Franklin RA, Abrams SL, Chappell W, Kempf CR, Basecke J, Stivala F, Donia M, Fagone P, Nicoletti F, Libra M, Ruvolo P, Ruvolo V, Evangelisti C, Martelli AM, McCubrey JA,

Roles of the Ras/Raf/MEK/ERK pathway in leukemia therapy, Leukemia 25 (2011) 1080–1094. [PubMed: 21494257]

[29]. Fruman DA, Rommel C, PI3K and cancer: lessons, challenges and opportunities, Nat. Rev. Drug Discov 13 (2014) 140–156. [PubMed: 24481312]

[30]. Juin P, Geneste O, Gautier F, Depil S, Campone M, Decoding and unlocking the BCL-2 dependency of cancer cells, Nat. Rev. Cancer 13 (2013) 455–465. [PubMed: 23783119]

[31]. Ley R, Balmanno K, Hadfield K, Weston C, Cook SJ, Activation of the ERK1/2 signaling pathway promotes phosphorylation and proteasome-dependent degradation of the BH3-only protein, Bim, J. Biol. Chem 278 (2003) 18811–18816. [PubMed: 12646560]

[32]. Luciano F, Jacquel A, Colosetti P, Herrant M, Cagnol S, Pages G, Auberger P, Phosphorylation of Bim-EL by Erk1/2 on serine 69 promotes its degradation via the proteasome pathway and regulates its proapoptotic function, Oncogene 22 (2003) 6785–6793. [PubMed: 14555991]

[33]. Korfi K, Smith M, Swan J, Somervaille TC, Dhomen N, Marais R, BIM mediates synergistic killing of B-cell acute lymphoblastic leukemia cells by BCL-2 and MEK inhibitors, Cell Death Dis 7 (2016) e2177. [PubMed: 27054332]

[34]. Rahmani M, Anderson A, Habibi JR, Crabtree TR, Mayo M, Harada H, Ferreira-Gonzalez A, Dent P, Grant S, The BH3-only protein Bim plays a critical role in leukemia cell death triggered by concomitant inhibition of the PI3K/Akt and MEK/ERK1/2 pathways, Blood 114 (2009) 4507–4516. [PubMed: 19773546]

[35]. Soares HP, Ming M, Mellon M, Young SH, Han L, Sinnet-Smith J, Rozengurt E, Dual PI3K/mTOR inhibitors induce rapid overactivation of the MEK/ERK pathway in human pancreatic cancer cells through suppression of mTORC2, Mol. Cancer Ther 14 (2015) 1014–1023. [PubMed: 25673820]

[36]. Sandhofer N, Metzeler KH, Rothenberg M, Herold T, Tiedt S, Groiss V, Carlet M, Walter G, Hinrichsen T, Wachter O, Grunert M, Schneider S, Subklewe M, Dufour A, Frohling S, Klein HG, Hiddemann W, Jeremias I, Spiekermann K, Dual PI3K/mTOR inhibition shows antileukemic activity in MLL-rearranged acute myeloid leukemia, Leukemia 29 (2015) 828–838. [PubMed: 25322685]

[37]. Choudhary GS, Al-Harbi S, Mazumder S, Hill BT, Smith MR, Bodo J, Hsi ED,Almasan A, MCL-1 and BCL-xL-dependent resistance to the BCL-2 inhibitor ABT-199 can be overcome by preventing PI3K/AKT/mTOR activation in lymphoid malignancies, Cell Death Dis. 6 (2015) e1593. [PubMed: 25590803]

[38]. Vanhaesebroeck B, Guillermet-Guibert J, Graupera M, Bilanges B, The emerging mechanisms of isoform-specific PI3K signalling, Nat. Rev. Mol. Cell Biol 11 (2010) 329–341. [PubMed: 20379207]

[39]. Yanagita T, Kobayashi H, Uezono Y, Yokoo H, Sugano T, Saitoh T, Minami S,Shiraishi S, Wada A, Destabilization of Na(v)1.7 sodium channel alpha-subunit mRNA by constitutive phosphorylation of extracellular signal-regulated kinase: negative regulation of steady-state level of cell surface functional sodium channels in adrenal chromaffin cells, Mol. Pharmacol 63 (2003) 1125–1136. [PubMed: 12695541]

[40]. Grandage VL, Gale RE, Linch DC, Khwaja A, PI3-kinase/Akt is constitutively active in primary acute myeloid leukaemia cells and regulates survival and chemoresistance via NF-kappaB, Mapkinase and p53 pathways, Leukemia 19 (2005) 586–594. [PubMed: 15703783]

[41]. Martelli AM, Evangelisti C, Chappell W, Abrams SL, Basecke J, Stivala F, Donia M, Fagone P, Nicoletti F, Libra M, Ruvolo V, Ruvolo P, Kempf CR, Steelman LS, McCubrey JA, Targeting the translational apparatus to improve leukemia therapy: roles of the PI3K/PTEN/Akt/mTOR pathway, Leukemia 25 (2011) 1064–1079. [PubMed: 21436840]

[42]. Rahmani M, Aust MM, Attkisson E, Williams DC Jr., Ferreira-Gonzalez A, Grant S, Dual inhibition of Bcl-2 and Bcl-xL strikingly enhances PI3K inhibition-induced apoptosis in human myeloid leukemia cells through a GSK3- and Bim-dependent mechanism, Cancer Res. 73 (2013) 1340–1351. [PubMed: 23243017]

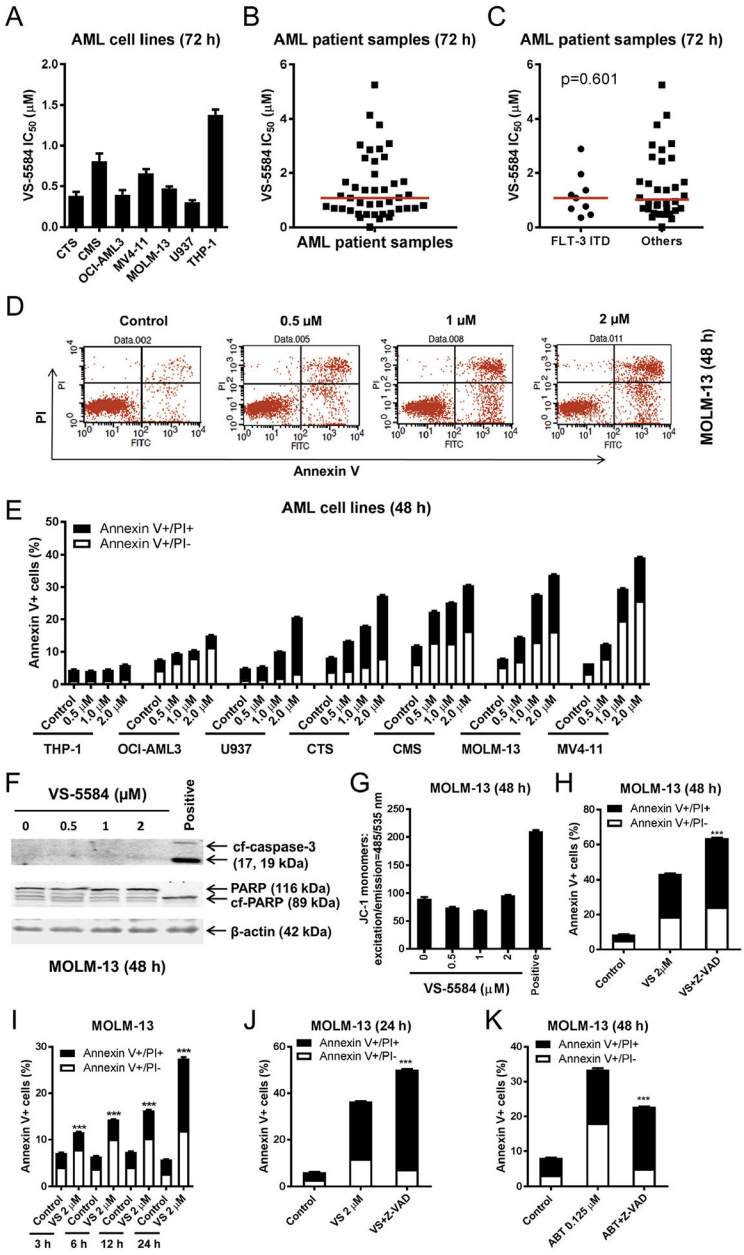

Fig. 1.

VS-5584 induces proliferation inhibition and caspase-independent cell death in AML cells. (A–C) AML cell lines and primary AML patient samples were treated with variable concentrations of VS-5584 for 72 h and viable cells were determined using MTT reagent. For AML cell lines, data are graphed as mean ± SEM from three independent experiments (panel A). For the patient samples, the IC_{50} values are means of duplicates from one experiment due to limited sample (panel B). Differences in VS-5584 IC_{50}s between FLT3-ITD vs. Non-FLT3 ITD was calculated using the Mann-Whitney *U* test (p = .601; panel C). The horizontal lines indicate the median. (D, E) AML cell lines were treated with VS-5584 for 48 h and then subjected to Annexin V-FITC/PI staining and flow cytometry analysis. Representative dot plots are shown in panel D. Mean percent Annexin V+ cells ± SEM are

shown in panel E. (F, G) MOLM-13 cells were treated with VS-5584 (or 100 nM CUDC-907 as a positive control) for 48 h. Western blots using whole cell lysates are shown (panel F). 5×10^5 cells were subjected to the JC-1 assay (panel G). (H) Annexin V-FITC/PI staining and flow cytometry analysis for MOLM-13 cells were treated for 48 h with 2 μM VS-5584 with or without 50 μM Z-VAD-FMK are shown. *** indicates $p < .001$. (I) Annexin V-FITC/PI staining and flow cytometry analysis results for MOLM-13 cells treated with 2 μM VS-5584 for 3, 6, 12, and 24 h are shown. *** indicates $p < .001$. (J, K) MOLM-13 cells were treated with 2 μM VS-5584 (24 h) or 0.125 mM ABT-199 (48 h) with or without 50 μM Z-VAD-FMK and then subjected to Annexin V-FITC/PI staining and flow cytometry analysis. ***indicates $p < .001$.

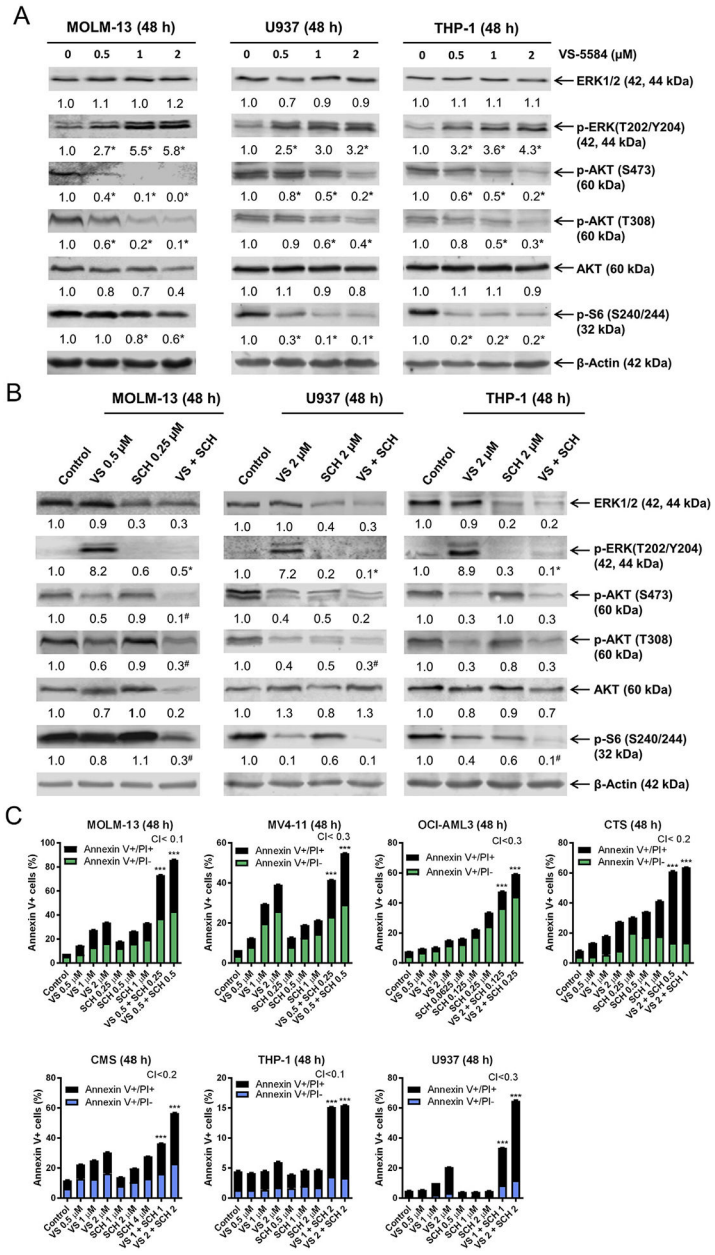

Fig. 2.

Inhibition of ERK enhances VS-5584-induced cell death in AML cell lines. (A, B) MOLM-13, U937, and THP-1 cells were treated with VS-5584 (VS), SCH772984 (SCH), or VS + SCH for 48 h. Whole cell lysates were subjected to Western blots which were probed with the indicated antibodies. Representative blots are shown; normalized densitometry measurements are indicated below the corresponding blot. For panel A, * indicates $p < .05$ compared to the control ($n = 3$). For panel B, #indicates $p < .05$ compared to individual drug treatment and * indicates $p < .05$ compared to VS treatment ($n = 3$, data not shown). (C) AML cell lines were treated with VS, SCH, or in combination for 48 h Annexin V-FITC/PI staining and flow cytometry analysis was performed. Mean percent Annexin V+ cells ±

SEM are shown. CI values were calculated using CompuSyn software. *** indicates $p < .001$.

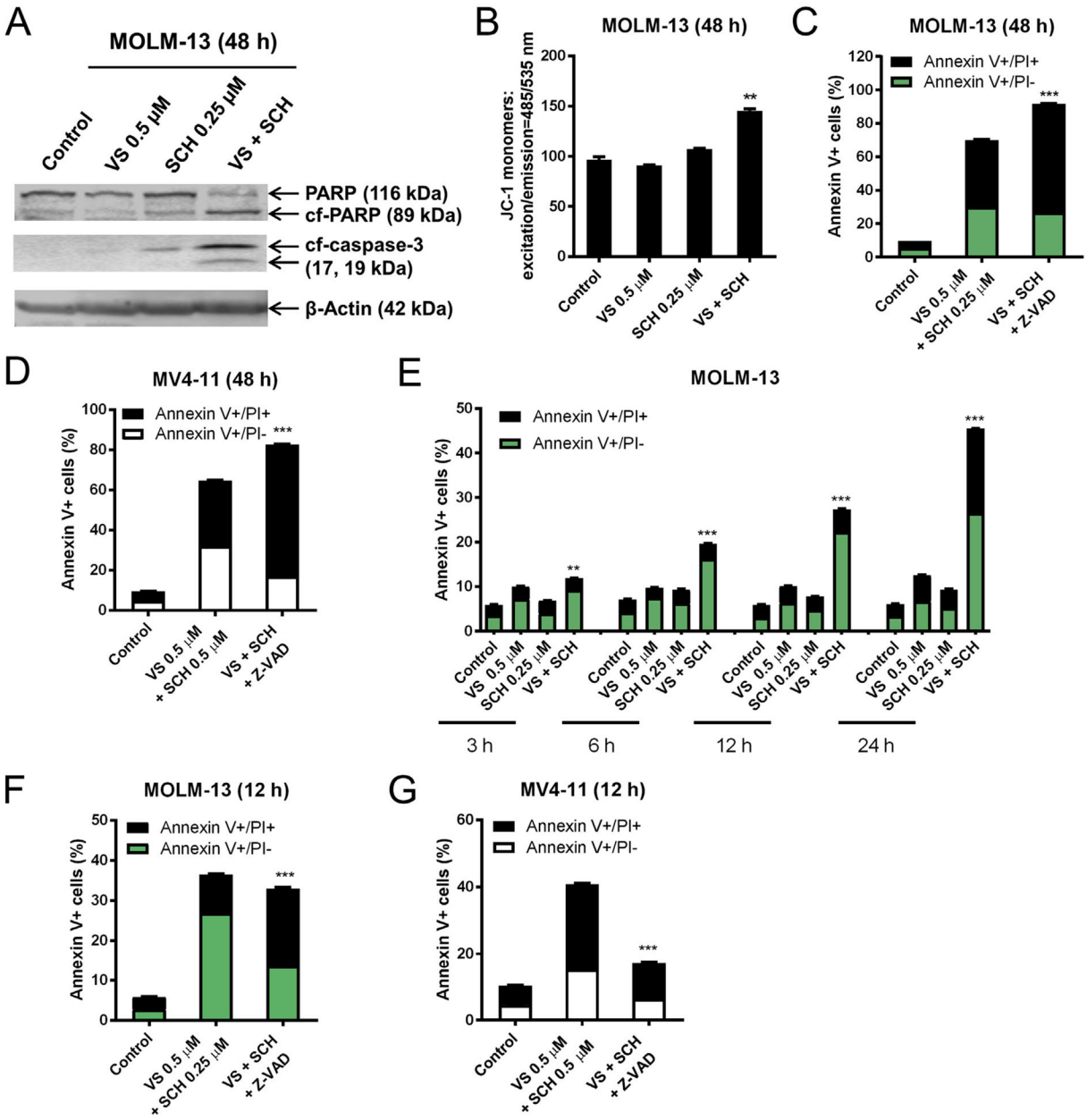

Fig. 3.

SCH772984 synergizes with VS-5584 to induce cell death in AML cell lines. (A, B) MOLM-13 cells were treated with VS-5584 (VS), SCH772984 (SCH), or VS + SCH for 48 h. Western blots probed with anti-PARP, -cf-caspase-3, and -β-actin are shown (panel A). 5 × 10^5 cells were subjected to the JC-1 assay (panel B). ** indicates $p < .01$. (C, D) MOLM-13 (panel C) and MV4–11 (panel D) cells were treated for 48 h with VS + SCH with or without 50 μM Z-VAD-FMK. Annexin V-FITC/PI staining and flow cytometry analysis results are shown. *** indicates $p < .001$. (E) MOLM-13 cells were treated for 48 h with 0.5 μM VS, 0.25 μM SCH, or 0.5 μM VS + 0.25 μM SCH for 3, 6, 12, or 24 h. Cell death was determined using Annexin V-FITC/PI staining and flow cytometry analysis. ** indicates $p < .01$ and *** indicates $p < .001$. (F, G) MOLM-13 (panel F) and MV4–11 (panel

G) cells were treated with VS + SCH with or without 50 μM Z-VAD-FMK for 12 h and then subjected to Annexin V-FITC/PI staining and flow cytometry analysis. *** indicates $p < .001$.

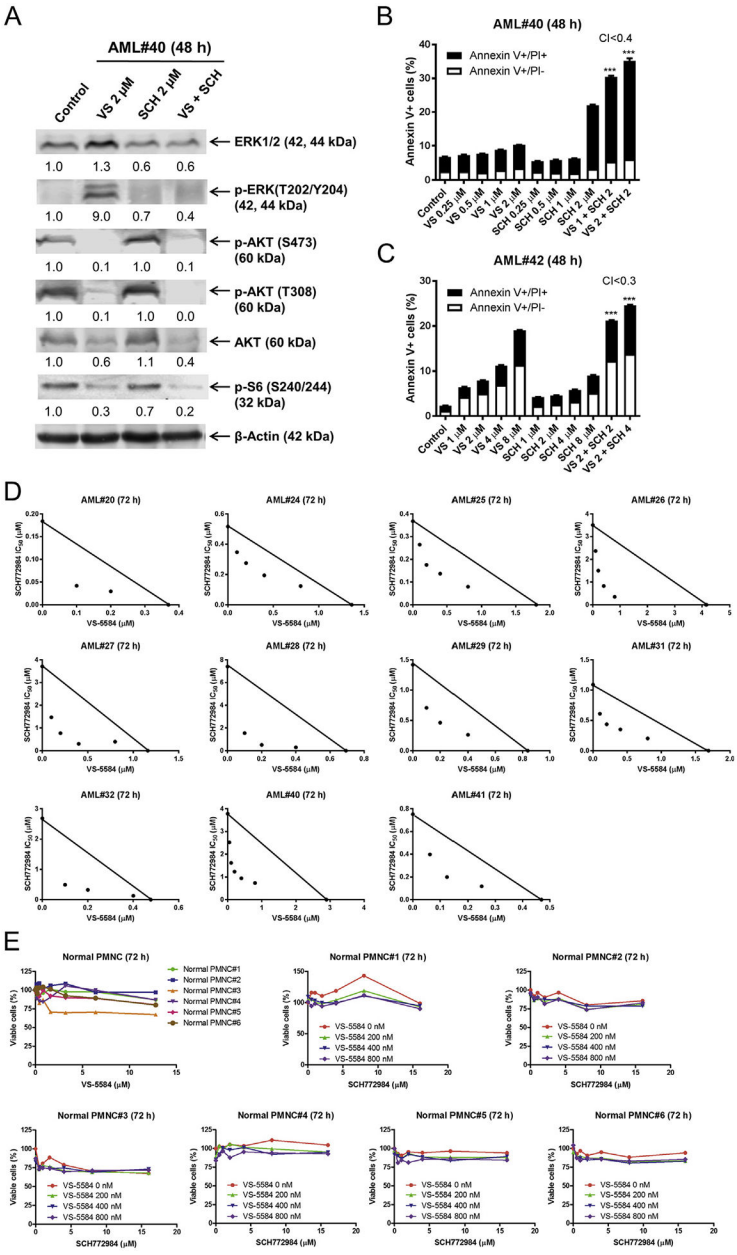

Fig. 4.

SCH772984 synergizes with VS-5584 in inducing cell death and proliferation inhibition in primary AML patient samples. (A) Primary AML patient sample AML#40 was treated with 2 μM VS-5584 (VS), 2 μM SCH772984 (SCH), or 2 μM VS + 2 μM SCH for 48 h. Whole cell lysates were subjected to Western blotting and probed with the indicated antibodies. Normalized densitometry measurement results are shown. Western blots were repeated once (due to limited sample) and one representative cropped blot is shown. (B, C) Primary AML patient samples (AML#40 and AML#42) were treated with VS, SCH, or in combination for 48 h. Mean percent Annexin V+ cells ± SEM are shown. CI values were calculated using CompuSyn software. *** indicates $p < .001$. (D) MTT assays were performed using primary AML patient samples treated with VS-5584 and SCH772984 for 72 h. The IC_{50} values are

means of duplicates from one experiment due to limited sample. Standard isobolograms are shown. The IC_{50} values for each drug are plotted on the axes; the solid line represents the additive effect, whereas the points represent the concentrations of each drug resulting in 50% inhibition of proliferation. Points falling below the line indicate synergism, whereas those above the line indicate antagonism. (E) Normal PMNCs were treated with VS-5584 and SCH772984, alone or in combination, for 72 h. Viable cells were determined using MTT assays.

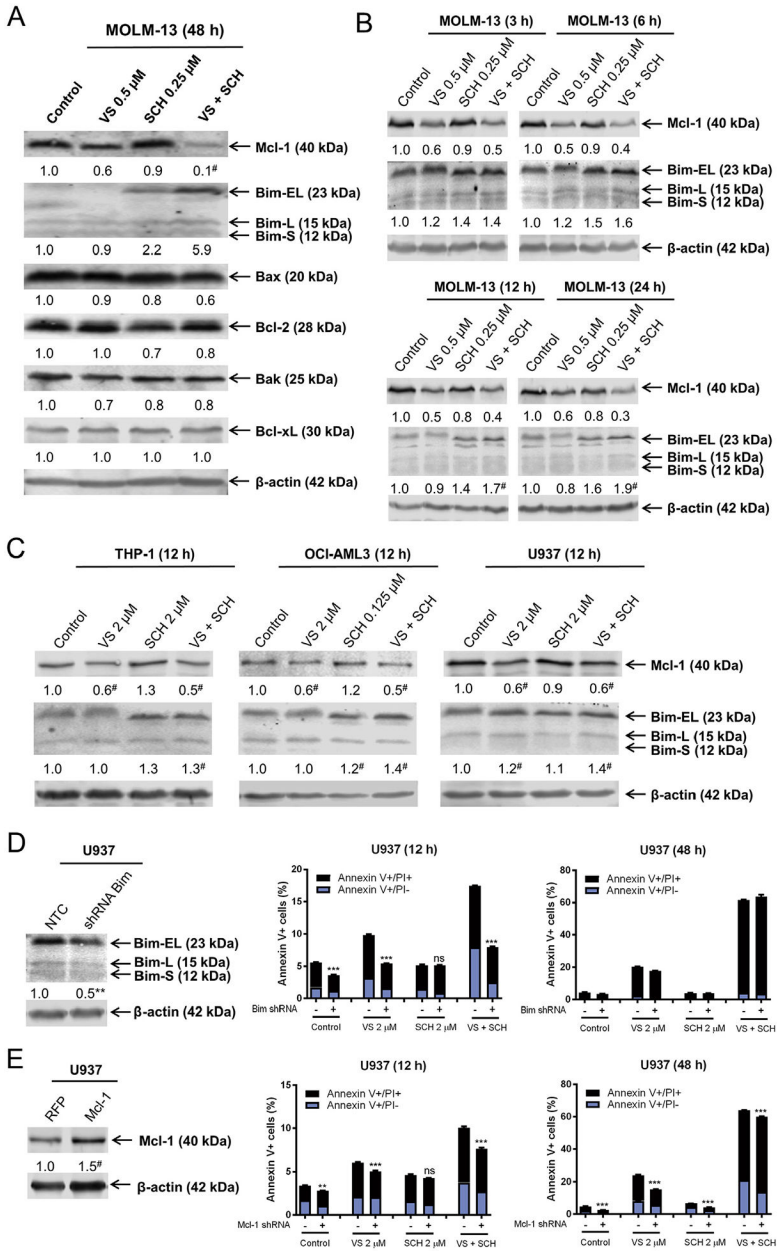

Fig. 5.

Downregulation of Mcl-1 and upregulation of Bim play an important role in cell death induced by the combination of VS-5584 and SCH772984 in AML cells. (A, B) MOLM-13 cells were treated with VS-5584 (VS), SCH772984 (SCH), or VS + SCH for 48 h (panel A) or up to 24 h (panel B). Normalized densitometry measurements for the Western blots are shown. # indicates $p < .05$ compared to control ($n = 3$, data not shown). (C) THP-1, OCI-AML3, and U937 cells were treated with VS, SCH, or VS + SCH for 12 h. Representative Western blots are shown with the corresponding normalized densitometry measurements below. * indicates $p < .05$ compared to VS alone ($n = 3$, data not shown). (D, E) U937 NTC or Bim shRNA knockdown (panel D) or Mcl-1 or RFP overexpression (panel E) was confirmed by Western blotting. Normalized densitometry measurements are indicated. **

indicates $p < .01$ compared to NTC ($n = 3$), while # indicates $p < .05$ compared to RFP ($n = 3$). U937 NTC and Bim shRNA or U937 RFP and Mcl-1 cells were treated with VS, SCH, or VS + SCH for 12 h or 48 h and then subjected to Annexin V/PI staining and flow cytometry analysis. *** indicates $p < .001$.

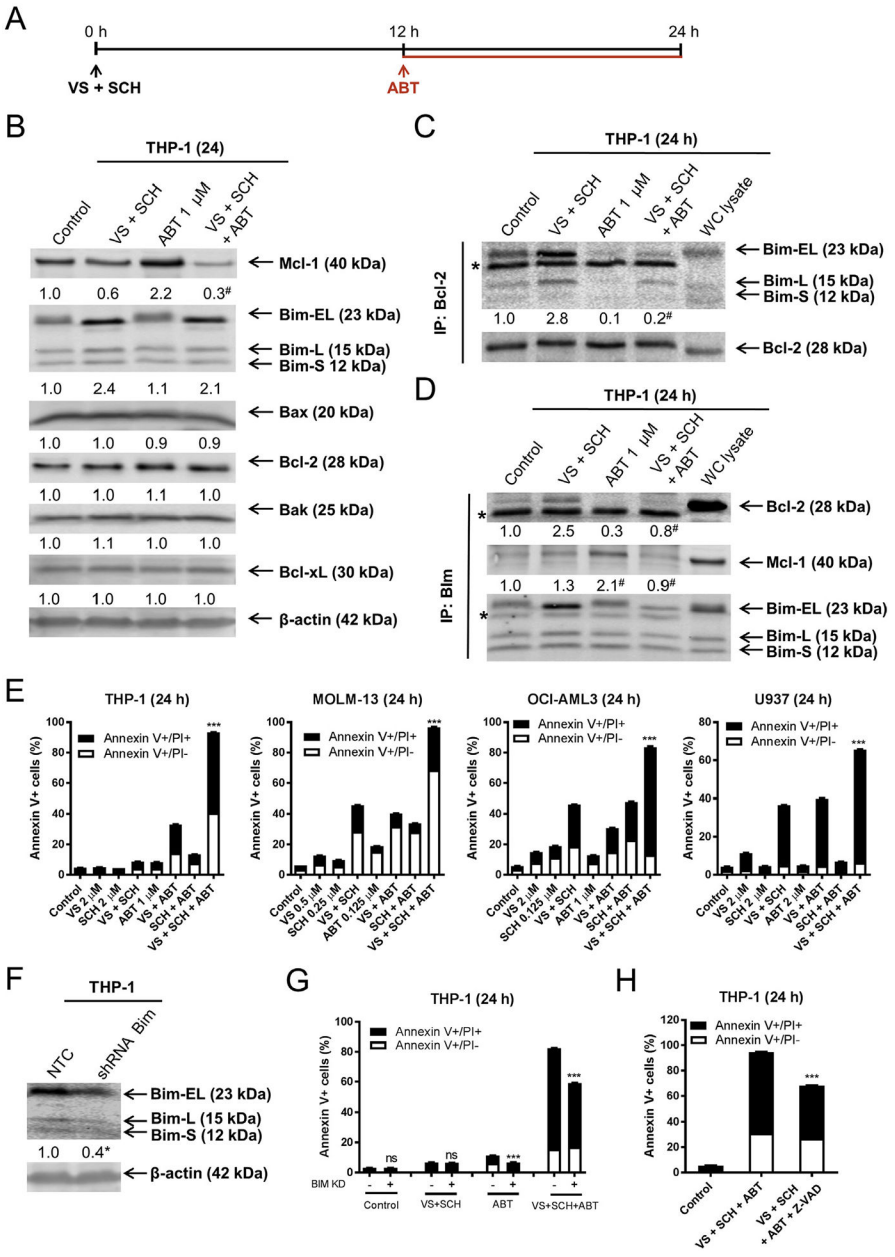

Fig. 6.

Upregulation of Bim and downregulation of Mcl-1 by combined VS-5584 and SCH772984 treatment is accompanied by increased association of Bim with Bcl-2. (A) Experimental outline for the combination of VS-5584 (VS), SCH772984 (SCH), and ABT-199 (ABT). (B) THP-1 cells were treated with VS + SCH for 12h, and then ABT was added for an additional 12 h. Representative Western blots, using whole cell lysates, are shown with the corresponding normalized densitometry measurements below. # indicates $p < .05$ compared to combined VS + SCH (n = 3, data not shown). (C, D) THP-1 cells were treated as shown in panel A. Bcl-2 (panel C) or Bim (panel D) was immunoprecipitated from whole cell lysates. Western blots were probed with anti-Mcl-1, Bim, or Bcl-2 antibody. The fold changes for Bcl-2, Mcl-1 and Bim densitometry measurements, compared to no drug

treatment control, are indicated. For panel C, # indicates $p < .05$ compared to combined VS + SCH (n = 3, data not shown). For panel D, # indicates $p < .05$ compared to VS + SCH (Bcl-2 blot) or ABT alone (Mcl-1 blot). (E) THP-1, MOLM-13, OCI-AML3, and U937 cells were treated as shown in panel A. Annexin V-FITC/PI staining and flow cytometry analysis results are shown. *** indicates $p < .001$. (F, G) THP-1 cells infected with NTC or Bim shRNA lentivirus were subjected to Western blotting and probed with the indicated antibodies. The fold changes for the Bim densitometry measurements, normalized to β-actin and then compared to no drug treatment control, are indicated (panel F). * indicates $p < .05$ compared to NTC (n = 3, data not shown). THP-1 NTC and Bim shRNA cells were treated as shown in panel A and subjected to Annexin V/PI staining and flow cytometry analysis (panel G). *** indicates $p < .001$. (H) In the presence or absence of 50 μM Z-VAD-FMK, THP-1 cells were pretreated with VS + SCH for 12 h, then ABT-199 was added for an additional 12 h, and then subjected to Annexin V/PI staining and flow cytometry analysis. *** indicates $p < .001$.

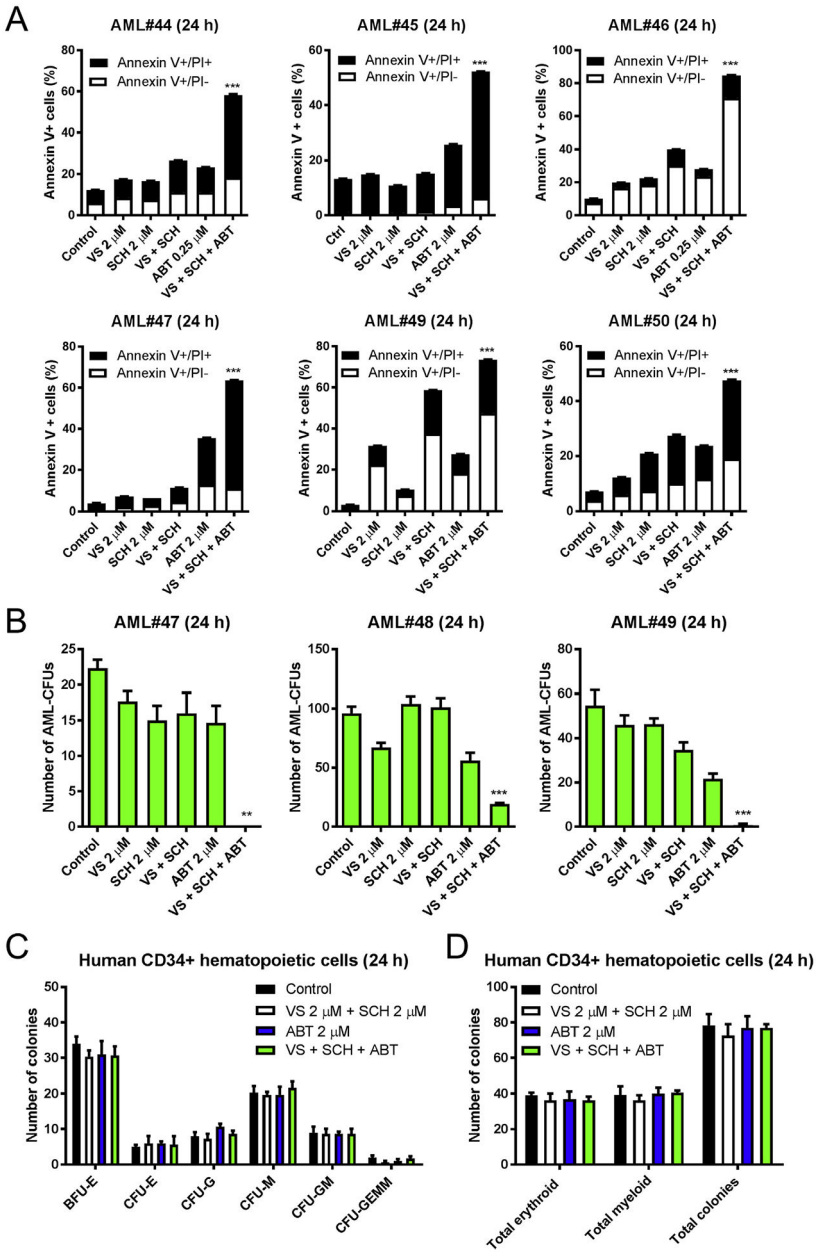

Fig. 7.

The combination of VS-5584, SCH772984, and ABT-199 shows superior antileukemic activities against primary AML blasts but spares normal hematopoietic progenitor cells. (A) Primary AML patient samples (n = 6) were pretreated with VS-5584 (VS) and SCH772984 (SCH) alone or in combination for 12 h and then ABT-199 was added for an additional 12 h. Mean percent Annexin V+ cells ± SEM are shown. *** indicates $p < .001$. (B) Primary AML patient samples (n = 3) were cultured with VS, SCH, and ABT-199, alone or in combination as described in panel A, for 24 h and then plated in methylcellulose and incubated for 2 weeks. The number of surviving AML cells capable of generating leukemia colonies (AML-CFUs) was enumerated. Data are presented as mean ± SEM. ** indicates $p < .01$ and *** indicates $p < .001$. (C, D) Human CD34+ cord blood cells were treated with

VS, SCH, and ABT-199, alone or in combination, as described in panel A. Cells were plated in methylcellulose and incubated for 2 weeks. The number of surviving hematopoietic cells capable of generating colonies was enumerated. The number of BFU-E, CFU-E, CFU-G, CFU-M, CFU-GM, and CFU-GEMM is presented as mean ± SEM (panel C). Total erythroid and myeloid colonies are presented as mean ± SEM (panel D).

Table 1

Patient characteristics of primary AML patient samples.

Patient	Gender	Age (year)	Disease status	FAB subtype	Cytogenetics	Blast purity (%)	Gene mutation
#1	M	17	Newly diagnosed	M2	46, XY	68.5	CEBPA double mutation
#2	F	76	Newly diagnosed	M5	46, XX	84.5	dupMLL, CEBPA signal mutation
#3	M	52	Newly diagnosed	M4	46, XY	96	DEK-CAN
#4	M	65	Newly diagnosed	M5	47, XY, add(7q), −16, −17, +marx3	76	
#5	M	43	Newly diagnosed	M2	46, XY, t(8;21)(q22;q22)	48	AML1-ETO
#6	M	50	Newly diagnosed	M2	45, X, −Y, t(8;21)(q22;q22), del(11q)	46	AML1-ETO
#7	M	12	Newly diagnosed	M3	46, XY, t(15;17)(q22;q21)	92.5	PML-RARα
#8	M	74	Newly diagnosed	M5	47, XY,+8	95	FLT-3 ITD, NPM-1, DNMT3A
#9	M	19	Newly diagnosed	M2	45, X, −Y, t(8;21)(q22;q22), del(9q)	47	AML1-ETO
#10	M	25	Newly diagnosed	M3	46, XY, t(15;17)(q22;q21)	94	PML-RARα
#11	M	48	Relapsed	M2	46, XY, t(7;11)(p15;p15)	39.5	FLT-3 ITD
#12	F	9	Newly diagnosed	M1	NA	93.5	
#13	F	50	Relapsed	M2	46, XX	81	CEBPA double mutation
#14	F	7	Newly diagnosed	M4	46, XX, t(11;20)(p15;q11)/46, idem, del(9) (q22)	83	EVI1
#15	F	52	Newly diagnosed	M3	46, XX, t(15;17)(q22;q21)	90	PML-RARα
#16	M	38	Newly diagnosed	M3	47, XY, add(1p), t(15;17)(q22;q21), +14	95	PML-RARα
#17	M	34	Newly diagnosed	M2	46, XY	29	FLT-3 ITD, dupMLL
#18	F	51	Newly diagnosed	M5	46, XX	82	
#19	M	48	Newly diagnosed	M5	46, XY	42	IDH2, DNMT3A
#20	F	77	Newly diagnosed	M4	46, XX	50	
#21	F	44	Newly diagnosed	M3	46, XX, t(15;17)(q22;q21)	89	PML-RARα
#22	F	12	Newly diagnosed	M2	47, XX, +10	80	FLT-3 ITD, CEBPα single mutation
#23	F	60	Newly diagnosed	M5	46, XX	69.5	
#24	F	32	Newly diagnosed	M4	46, XX, del(9q)	27	CEBPA double mutation
#25	F	65	Newly diagnosed	M5	46, XX	91	Flt-3 ITD, NPM-1
#26	M	18	Newly diagnosed	M3	46, XY, t(15;17)(q22;q21)	95	PML-RARα
#27	M	64	Newly diagnosed	M4	46, XY	69	
#28	M	59	Newly diagnosed	M2	46, XY	82	HOX11

Patient	Gender	Age (year)	Disease status	FAB subtype	Cytogenetics	Blast purity (%)	Gene mutation
#29	F	75	Newly diagnosed	M4	46, XX, +8	91	
#30	F	54	Newly diagnosed	M5	46, XX	64	MLL-AF6
#31	F	48	Newly diagnosed	M6	45, XX, del(3q), −7	39	
#32	F	35	Newly diagnosed	M2	45, X, −X, t(8;21)(q22;q22)	22.5	AML1-ETO, FLT-3 ITD
#33	F	64	Newly diagnosed	M4	NA	91	dupMLL, FLT-3 ITD, IDH1
#34	M	76	Newly diagnosed	M4	46, XY	95.5	
#35	F	46	Newly diagnosed	M2	46, XX	64.5	MDS
#36	F	50	Newly diagnosed	M4	46, XX	91.5	FLT-3 ITD, NPM-1, DNMT3A
#37	F	69	Newly diagnosed	M1	46, XX	91.5	
#38	F	59	Newly diagnosed	M4	46, XX	82.0	CEBPA double mutation
#39	F	14	Newly diagnosed	M2	46, XX	34.0	CEBPA double mutation
#40	M	65	Newly diagnosed	M4	46, XY	86.0	FLT-3 ITD, DNMT3A, IDH2
#41	M	55	Newly diagnosed	M3	46, X, −Y, t(15;17)(q22;q21)	93.0	PML-RARα
#42	M	27	Newly diagnosed	M3	46, X, Y, t(15;17)(q22;q21)	94,0	FLT-3 ITD, PML-RARα
#43	F	66	Relapsed	M4	45, XX, −7	48.0	
#44	M	19	Newly diagnosed	M4	46, XY	63	CEBPA, c-Kit, NRAS, GATA2, Flt3 S451F
#45	M	77	Newly diagnosed	M4	NA	NA	NA
#46	M	53	Relapsed	M2	NA	98.0	
#47	F	62	Newly diagnosed	M1	NA	98.50	RUNX1 、BCOR 、FLT3
#48	F	4	Newly diagnosed	M2	46, XX, t(8;21)(q22;q22)	26.00	N-RAS
#49	F	55	Newly diagnosed	M1	46, XX	98.00	K-RAS
#50	F	38	Newly diagnosed	M4	46, XX	87.00	FLT3-ITD 、DNMT3A